Quantifying temporal bone morphology of great apes and humans: an approach using geometric morphometrics

Charles A. Lockwood,[1] John M. Lynch[2] and William H. Kimbel[1]

[1]*Department of Anthropology & Institute of Human Origins, and* [2]*Barrett Honors College & Institute of Human Origins, Arizona State University, Tempe, AZ 85287, USA*

Abstract

The hominid temporal bone offers a complex array of morphology that is linked to several different functional systems. Its frequent preservation in the fossil record gives the temporal bone added significance in the study of human evolution, but its morphology has proven difficult to quantify. In this study we use techniques of 3D geometric morphometrics to quantify differences among humans and great apes and discuss the results in a phylogenetic context. Twenty-three landmarks on the ectocranial surface of the temporal bone provide a high level of anatomical detail. Generalized Procrustes analysis (GPA) is used to register (adjust for position, orientation and scale) landmark data from 405 adults representing *Homo*, *Pan*, *Gorilla* and *Pongo*. Principal components analysis of residuals from the GPA shows that the major source of variation is between humans and apes. Human characteristics such as a coronally orientated petrous axis, a deep mandibular fossa, a projecting mastoid process, and reduced lateral extension of the tympanic element strongly impact the analysis. In phenetic cluster analyses, gorillas and orangutans group together with respect to chimpanzees, and all apes group together with respect to humans. Thus, the analysis contradicts depictions of African apes as a single morphotype. Gorillas and orangutans lack the extensive preglenoid surface of chimpanzees, and their mastoid processes are less medially inflected. These and other characters shared by gorillas and orangutans are probably primitive for the African hominid clade.

Key words geometric morphometrics; hominids; hominoids; relative warp analysis; thin-plate spline analysis.

Introduction

The temporal bone participates in forming the neurocranium, articulates with the mandible, houses the apparatus of hearing and balance, and is one surface of attachment for masticatory, neck and throat musculature. Its complex array of morphology is therefore relevant to several functional systems and dense with potential phylogenetic information. Moreover, it is often preserved in the hominid[1] fossil record. Palaeoanthropologists have frequently examined the temporal bone for taxonomic and phylogenetic evidence.

Recognition of the value of temporal bone morphology in hominid systematics goes back to the first fossil hominid discoveries, and especially Weidenreich (1943), who characterized the distinctive, autapomorphic form of the *Homo erectus* temporal bone. Since then, qualitative studies of the temporal bone have resulted in detailed descriptions of this anatomical region, but comparisons among them are difficult because morphology can be portrayed or categorized differently by different authors (Weidenreich, 1943, 1948; Le Gros Clark, 1947; Tobias, 1967, 1991; Clarke, 1977; Olson, 1981, 1985; White et al. 1981; Kimbel et al. 1984; Picq, 1984, 1985, 1990; Kimbel & White, 1988; Hill et al. 1992; Kimbel & Rak, 1993; Lockwood & Tobias, 1999; Sherwood et al. 2002). The quantitative shape of the temporal bone has been expressed mainly by dimensions and angles of the mandibular fossa (e.g. Ashton & Zuckerman, 1954; Tobias, 1967, 1991; Wood,

1991) or the cranial base as a whole (Dean & Wood, 1981, 1982). Martinez & Arsuaga (1997) recently integrated different elements of the temporal bone in a univariate study applied to Pleistocene *Homo*. The combination of detailed anatomical observations with univariate treatment of particular characters sets the stage for a detailed multivariate study of temporal bone morphology.

In this study, we use three-dimensional landmarks on the ectocranial surface of the temporal bone to quantify the expression of features that have thus far been discussed qualitatively or in a univariate context, and to identify novel aspects of temporal bone shape that distinguish hominid taxa. To quantify overall shape variation, principal components analysis (PCA) is conducted on residuals from generalized Procrustes analysis (this two-step procedure is equivalent to relative warp analysis). Thin-plate spline analysis (TPSA) is used to illustrate differences between taxa (O'Higgins & Jones, 1998). Together, PCA of Procrustes residuals and TPSA provide an excellent combination of techniques for the two purposes of morphometric comparative studies: first to *detect*, and then to *describe*, differences among taxonomic units.

These methods have received increasing use by anatomists and physical anthropologists. After initial studies of two-dimensional data (e.g. Lynch et al. 1996; Wood & Lynch, 1996; Yarroch, 1996), the collection of three-dimensional data has become popular – though such data are sometimes analysed or visualized after reducing it by one dimension (de Leon & Zollikofer, 2001; O'Higgins et al. 2001; Penin & Berge, 2001; Hennessy & Stringer, 2002; Rosas & Bastir, 2002)[2]. These studies have illustrated the applicability of geometric morphometrics to the cranium as a whole, the face in particular, and specific anatomical contours. A study of the temporal bone offers the opportunity to examine the utility of these methods when applied to a relatively more complex shape.

Although we evaluate the power of geometric morphometrics by comparing the results to previously recognized anatomical characters, many of our results are novel observations that bear on questions of great ape systematics and phylogeny. It has been suggested that cranial shape variation is not congruent with the most widely supported molecular phylogeny of hominids, and hence that cranial morphology is misleading in phylogenetic analysis (Collard & Wood,

Table 1 Hominid samples included in this study

Species or subspecies	Males	Females	Source
Pongo p. pygmaeus	17	20	NMNH
Pongo p. abellii	5	5	NMNH
Gorilla g. gorilla	36	36	CMNH, PCM
Gorilla g. beringei	11	6	NMNH, RMCA
Pan t. troglodytes	39	39	CMNH, PCM
Pan t. schweinfurthii	20	20	RMCA
Pan t. verus	24	24	PM
Pan paniscus	19	23	RMCA
Homo sapiens	32	29	CMNH

Abbreviations: CMNH – Cleveland Museum of Natural History; RMCA – Royal Museum for Central Africa, Tervuren, Belgium; NMNH – National Museum of Natural History, Washington, DC, USA; PCM – Powell-Cotton Museum, Birchington, UK; PM – Peabody Museum, Harvard University.

2000). Continued morphological study is a way of testing this hypothesis.

In this paper, we compare hominid taxa by extracting information from an important source of morphological evidence and by applying quantitative methods specifically designed for comparisons of shape. Some results based on smaller samples have been presented in abstract form (Lockwood et al. 2000). We focus on the systematic implications of temporal bone morphology, and especially differences among extant hominid genera. This will provide the context for addressing questions concerning hominid species diversity and the fossil record in subsequent publications, and exploring the functional basis for the evolution of human temporal bone form.

Materials and methods

Samples

In the present study we sampled nine different populations of extant hominids, representing five different species (in a conservative taxonomy). Table 1 summarizes sample sizes and composition. Groupings are based on subspecies classifications that essentially correspond to geographical populations. These include *Gorilla gorilla gorilla*, *G. g. beringei*, *Pan paniscus*, *P. troglodytes troglodytes*, *P. t. schweinfurthii*, *P. t. verus*, *Pongo pygmaeus pygmaeus*, *P. p. abellii* and *Homo sapiens* (a cadaver-based African-American sample). Non-human specimens are from wild-shot individuals. Information was recorded on various developmental

Table 2 Definitions of landmarks used in this study[1]

1	Intersection of the infratemporal crest and sphenosquamosal suture
2	Most lateral point on the margin of foramen ovale[2]
3	Most anterior point on the articular surface of the articular eminence
4	Most inferior point on entoglenoid process
5	Most inferior point on the medial margin of the articular surface of the articular eminence
6	Midpoint of the lateral margin of the articular surface of the articular eminence
7	Centre of articular eminence[3]
8	Deepest point within mandibular fossa[4]
9	Most inferior point on the postglenoid process
10	Point on anterior margin of tympanic element that is closest to carotid canal
11	Apex of the petrous part of the temporal bone
12	Most posterolateral point on the margin of the carotid canal entrance
13	Most lateral point on the vagina of the styloid process (whether process is present or absent)
14	Most lateral point on the margin of the stylomastoid foramen
15	Most lateral point on the jugular fossa
16	Centre of the inferior tip of the mastoid process
17	Most inferior point on the external acoustic porus
18	Most inferolateral point on the tympanic element of the temporal bone
19	Point of inflection where the braincase curves laterally into the supraglenoid gutter, in coronal plane of mandibular fossa
20	Point on lateral margin of zygomatic process of the temporal bone at the position of the postglenoid process
21	Auriculare
22	Porion
23	Asterion

[1]Definitions for standard craniometric landmarks follow Braeuer (1988).

[2]This is the only landmark not on the temporal bone that was included in the analysis. Foramen ovale provides a highly replicable landmark near the medial margin of anterior portion of temporal bone and is preferred here to a more arbitrary point located on, for example, the sphenosquamosal suture.

[3]The centre of the articular eminence was determined instrumentally with calipers prior to digitizing. The horizontal distance covered by the eminence was used for this purpose.

[4]If there was no 'deepest point' evident in the mandibular fossa, the centre of the fossa was determined instrumentally, as with the centre of the articular eminence.

indicators. The present study is directed towards adult individuals. Young adults (individuals with M3 erupted but with an unfused spheno-occipital synchondrosis) are included in the analysis because differences between them and full adults are negligible relative to species differences.

Data acquisition

Our list of 23 temporal bone landmarks is presented in Table 2 and illustrated in Fig. 1. These landmarks were chosen to record as many clearly defined and repeatably identifiable ectocranial points as possible. Data were recorded with a Microscribe 3DX portable digitizer, which obtains coordinates for each landmark relative to the centre of its base. Each specimen was mounted in a stable, elevated ring so that all landmarks could be obtained in a single series. No landmarks are missing for any specimen included in this study. An examination of measurement error is provided below.

Geometric morphometrics

As landmark-based morphometrics has gained significant support among anatomists, an in-depth presentation of the background to the methodology will not be given here. Readers unfamiliar with the techniques are directed to Lynch et al. (1996), O'Higgins & Jones (1998), O'Higgins (2000) and O'Higgins et al. (2001) for non-specialist descriptions, while Bookstein (1991), Dryden & Mardia (1998) and a number of the papers in Marcus et al. (1996) cover the more technical aspects of these methods. Statistical justifications for the use of these methods are presented in Rohlf (1999, 2000a,b).

Geometric morphometric techniques allow the decomposition of the form of an object into size and shape. Size is retained as 'Centroid Size' (CS), the sum of squared Euclidian distances from each landmark to the centroid of the shape. For this study, shape is defined as the information remaining once location, size and rotational effects are removed via generalized Procrustes analysis (GPA) – a method of superimposition
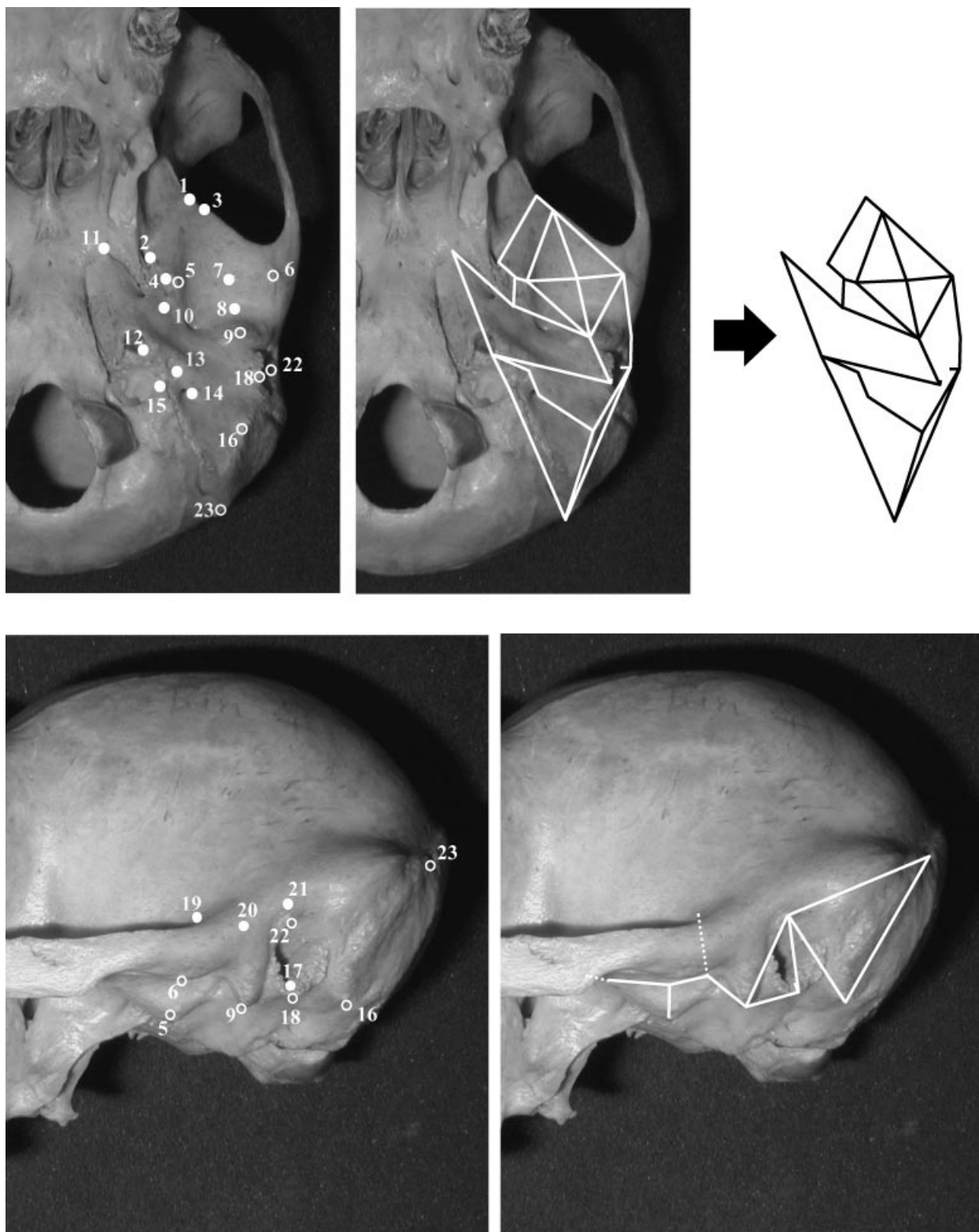
Fig. 1 Landmarks used in this study, labelled on a chimpanzee cranium in inferior view (above) and lateral view (below). Numbers correspond to those given in Table 2. Some landmarks (open circles) are labelled in both views. Temporal bone form is illustrated by use of wireframe diagrams linking landmarks, as shown in the panels on the right.

that seeks to minimize the sum of squared distances between equivalent landmarks across a sample of specimens (Rohlf & Slice, 1990; Goodall, 1991). The Procrustes residuals from the grand mean (in three dimensions, three residuals per landmark per specimen) then form the basis for all subsequent statistical analyses. These residuals are not entirely 'size free' but retain shape information that is due to allometry.

In a similar manner to more traditional morphometric data, the Procrustes residuals can be analysed using standard multivariate techniques, such as PCA or canonical variates analysis. Principal components analysis of the Procrustes residuals is sometimes referred to as 'relative warp analysis', and this is our method of choice for studying overall variation. The same methodology is referred to as 'simple tangent space projection' by O'Higgins & Jones (1998) because registered coordinates are projected into a plane tangent to the high-dimensional space occupied by landmark data. This morphospace, referred to as Kendall's shape space, is non-linear (Kendall, 1984). Tangent projection is necessary for statistical analysis (Dryden & Mardia, 1993). For biological shapes, which occupy a tiny part of Kendall's shape space, different methods of projection provide virtually identical results (O'Higgins & Jones, 1998).

While GPA provides the basis for quantifying and testing patterns of shape variation, the depiction of shape change is best achieved using thin-plate splines (see Bookstein, 1989). Thin-plate spline analysis allows the deformation of a reference form onto another form, resulting in a grid that demonstrates how homologous landmarks on one form are mapped onto the other. Shape difference is thus modelled using a depiction of one form as a continuous deformation of the other. Such grids make it relatively easy to visualize shape differences. For a more detailed discussion of TPSA and its connection with GPA see Bookstein (1989) and – on a less technical level – Lynch et al. (1996).

Intra-observer error

The Microscribe 3DX has a reported accuracy of ±0.23 mm (Immersion Corporation, 1998). To gauge the degree of intra-observer error in recording our landmarks, C.A.L. digitized four specimens each of *H. sapiens* and *P. troglodytes* three times. The first and second sets of landmarks for each specimen were recorded 2 years apart (at the beginning and end of data collection for

all other individuals), while only a few days separated the second and third sets of landmarks. Repeats from the same individual were superimposed using GPA to identify which landmarks had the greatest error. This procedure showed that the amount of error for individual landmarks is for the most part specific to individual crania. 'Floating' (instrumentally determined) landmarks, such as the centre of the articular eminence, are not more erratic than those located on specific bony features (such as the apex of the entoglenoid process).

In the process of analysing the data, it was immediately obvious that a mistake had been made in data collection for one human specimen, with one landmark accidentally replaced by the repeat of another. This individual was deleted from subsequent analyses of repeatability. Examination of outliers was conducted to ensure that extreme positions of individuals were not due to errors in data collection such as an inadvertent exchange of landmark order.

The overall effect of landmark error, which is most relevant for the analyses conducted below, was assessed by comparing Euclidean distances obtained between repeats of the same individuals to those obtained between different individuals. These were calculated from all 62 meaningful principal components generated in an analysis of 23 landmarks[3]. Results are shown in Fig. 2. In no case did the Euclidean distances between repeated measurements of the same individual exceed the distance between any two different individuals. As expected, the sets of landmarks collected only days apart were more similar in every case than either was to the initial data collection 2 years prior. These results demonstrate that intra-observer error is unlikely to affect interpretations of individual specimen affinity, and certainly not differences on the order of those found between species.

An informal analysis of repeated measurements of orangutan individuals suggests problems in the reliable identification of the landmark asterion when sutures are fused and strong temporonuchal crests occur. We therefore omit asterion from the analyses in this paper, in which orangutans and gorillas play a major role.

Defining the morphospace

Two series of analyses were conducted. The first is of all hominid taxa, and the second excludes humans. In each case, 22 landmarks (excluding asterion) for all specimens were superimposed using GPA, and principal
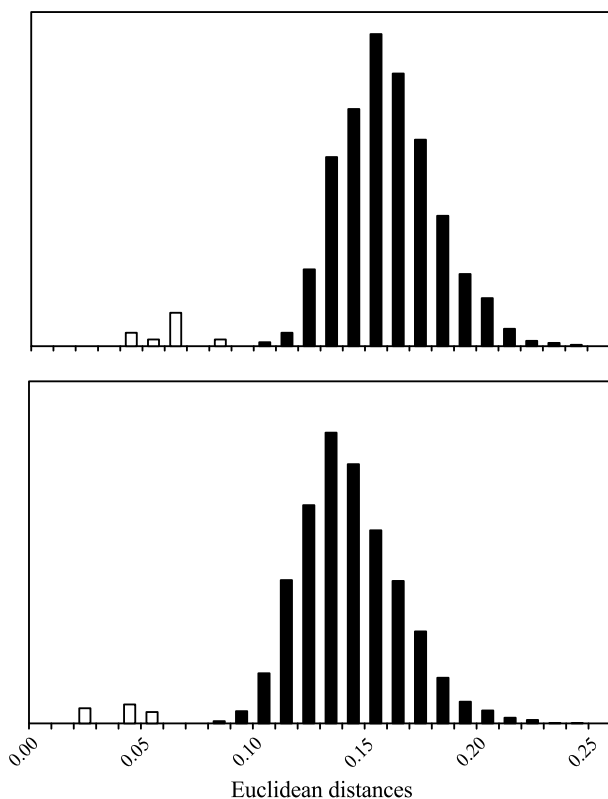
Fig. 2 Analysis of intra-observer error. Frequency distributions of all Euclidean distances among 59 specimens of *H. sapiens* (top panel) and among 78 specimens of *Pan troglodytes troglodytes* (bottom panel) are shown in black. White columns show the distributions for Euclidean distances between repeated sets of landmarks for the same individuals. The latter are not to scale and are exaggerated to illustrate their position relative to differences between individuals.

components (PCs) calculated based on GPA residuals. Plots of paired PCs were examined for separation among taxa. To summarize the phenetic relationships among taxa, Euclidean distances between group PC means (species or subspecies, as designated in Table 1) were clustered using unweighted pair-group averages (UPGMA). Principal components representing 99% of the original variance were used for this purpose.

Principal component analysis and TPSA were carried out using *Morphologika* (O'Higgins & Jones, 1998), while cluster analysis made use of *Statistica* (Release 5.5, Statsoft, Inc.). *Morphologika* provides a graphical link of schematic 'wireframe' diagrams to bivariate plots of principal components. For any location in the graph, the location of all landmarks (and therefore the shape of a wireframe) can be calculated from the eigenvectors of the chosen principal components. All other principal components are held constant in this

procedure (see O'Higgins & Jones, 1998, for more information). This program feature allows relatively easy determination of which landmarks, and therefore which qualitative features, impact each principal component. All morphological observations in the paper were first made using this technique.

An alternative method of studying shape variation is the use of TPSA between a reference form (the starting point for the thin-plate spline transformation) and target form (the endpoint of the transformation). For the purpose of illustrating shape differences in print, we used TPSA to describe the differences along each of the major principal components. While the resulting figures are in 2D, all analyses reflect 3D change. The designation of reference and target forms is arbitrary and not intended to convey the path of evolution.

Results

Principal component analysis of all hominids

Three PCs are necessary to illustrate the major differences among the four hominid genera studied here (Fig. 3). The first axis illustrates the pronounced difference between modern human temporal bone morphology and that of all great apes. The second axis primarily distinguishes gorillas and orangutans from chimpanzees and bonobos, and to a lesser extent separates the taxa within these two groups from each other. The third axis is driven by differences between orangutans and other taxa, and the fourth separates bonobos from chimpanzees. Further PCs contribute to resolving differences among populations within taxa.

There is a large amount of individual, intraspecific variation in temporal bone morphology, and this variation is captured by our analysis. Therefore, the first three PCs, which account for most interspecific variation, describe only 58.7% of the total variance in the data set (Table 3). There is no clear indication from descending eigenvalues at what point PCs become unimportant.

To illustrate the phenetic relationship of the hominids to each other, we conducted a cluster analysis of Euclidean distances among mean forms for each subspecies, based on 48 PCs (representing 99% of the original variance). Figure 4 illustrates the clustering of *Gorilla* and *Pongo* relative to *Pan* or *Homo*, consistent with plots of PC scores. The great apes together form a cluster distinct from humans, which are separated from the ape genera
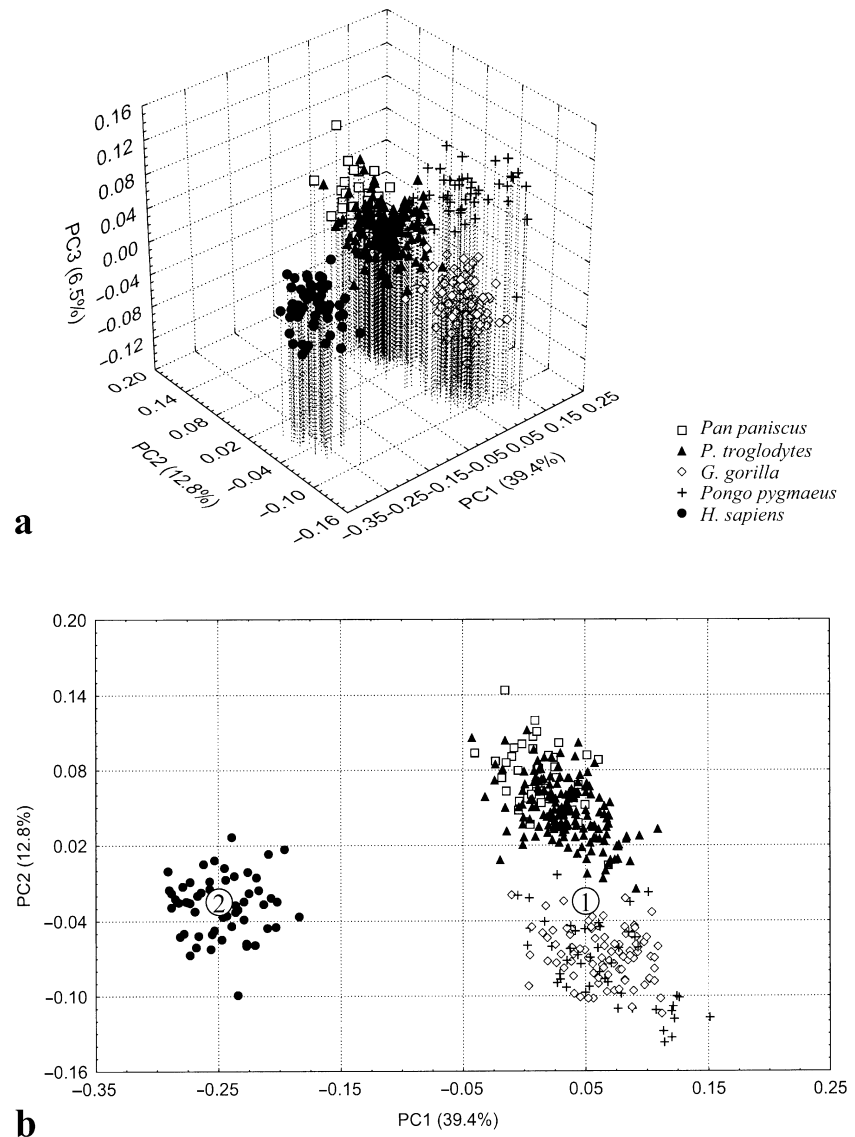
Fig. 3 PCA of all hominids. (a) The first three PCs summarize the differences among all species. (b) The analysis is dominated by the differences between humans and great apes, as described by PC1. The points marked '1' and '2' are the reference and target shapes for the thin-plate spline transformation illustrated in Figs 5 and 6.

by a distance much greater than those separating great ape species.

Thin-plate spline comparison: *H. sapiens* vs. great apes

The dramatic difference between humans and the great apes is illustrated in Figs 5 and 6, a thin-plate spline analysis based on the variation represented by PC1. In this case, a generic ape form is set as the reference form, and the modern human centroid is the target form. The 'generic ape' does not represent the centroid of all ape individuals, nor does it represent the ancestral condition for hominids. It was chosen simply to show changes along PC1.

While differences are calculated in three dimensions, they are most easily visualized in two dimensions.

Three spline planes are made available in *Morphologika*, and two of them are illustrated here, on different wireframe diagrams. The wireframe diagrams in Fig. 5 essentially represent inferior views of hominid temporal bones. In this view, the most basic difference between humans and great apes is that glenoid, tympanic and mastoid parts of human temporal bones are mediolaterally compressed. This shape difference gives rise to the narrowness of the posterior portion of the deformation grid, and contributes to the small overall area occupied by the temporomandidular joint. The broad anterior portion of the grid is related to the relatively coronal orientation of the human petrous element, commonly recognized to be apomorphic relative to the more sagittal orientation of other hominoids (e.g. Dean & Wood, 1981, 1982; Strait et al.

Table 3 Eigenvalues and distribution of variance for the first 10 components of each PCA

PC	Eigenvalue	Proportion of total variance (%)	Cumulative proportion (%)
Analysis of all hominid taxa			
1	0.012000	39.4	39.4
2	0.003880	12.8	52.2
3	0.001980	6.5	58.7
4	0.001210	4.0	62.7
5	0.001050	3.5	66.1
6	0.000898	3.0	69.1
7	0.000779	2.6	71.7
8	0.000674	2.2	73.9
9	0.000589	1.9	75.8
10	0.000539	1.8	77.6
Analysis excluding humans			
1	0.004870	24.3	24.3
2	0.002240	11.2	35.5
3	0.001310	6.5	42.0
4	0.001140	5.7	47.7
5	0.001110	5.6	53.2
6	0.000767	3.8	57.1
7	0.000704	3.5	60.6
8	0.000638	3.2	63.8
9	0.000588	2.9	66.7
10	0.000486	2.4	69.1

1997). Another clear apomorphy of humans is the reduced lateral extension of the tympanic element. Table 4 provides a more complete list of morphological traits and how they relate to differentiation along the PC axes.

The line extending laterally from the centre of the mandibular fossa terminates at a point on the side of the braincase. This perspective demonstrates very well that the human mandibular fossa is positioned mostly underneath the braincase. In the 'generic ape' wireframe, the mandibular fossa extends further laterally, and the highlighted segment is therefore shorter (i.e. the centre of the fossa is closer to the calvarial wall). This comparison is influenced primarily by *Gorilla* and *Pongo*; *Pan* is similar to *Homo*, as demonstrated below. Mediolateral variation in the position of the fossa is observed among species of fossil hominins (Tobias, 1991; Hill et al. 1992; Lockwood & Tobias, 1999; Sherwood et al. 2002).

The lateral view wireframe shown in Fig. 6 tracks the contours of the following structures from left to right: the articular eminence and entoglenoid process, the mandibular fossa, the postglenoid process, the tympanic element, and the mastoid process (see also Fig. 1). As in the inferior view, the grid is in a slightly different position within the temporal bone in each frame of the figure.

Human temporal bones have much more topographic relief than great ape temporal bones, as illustrated by the inferior extension of the mastoid process and the tympanic element, the great depth of the mandibular fossa, and the correspondingly steep posterior face of the articular eminence. Both the entoglenoid and the postglenoid processes are poorly developed inferiorly, and the entoglenoid process is orientated postero-inferiorly.

A deeper mandibular fossa in humans covaries with a strongly anteroposteriorly compressed preglenoid plane (see also Ashton & Zuckerman, 1954). The latter character is illustrated in the splines from inferior view. The inferior extension of the tympanic element in humans corresponds to the presence of a crest along its
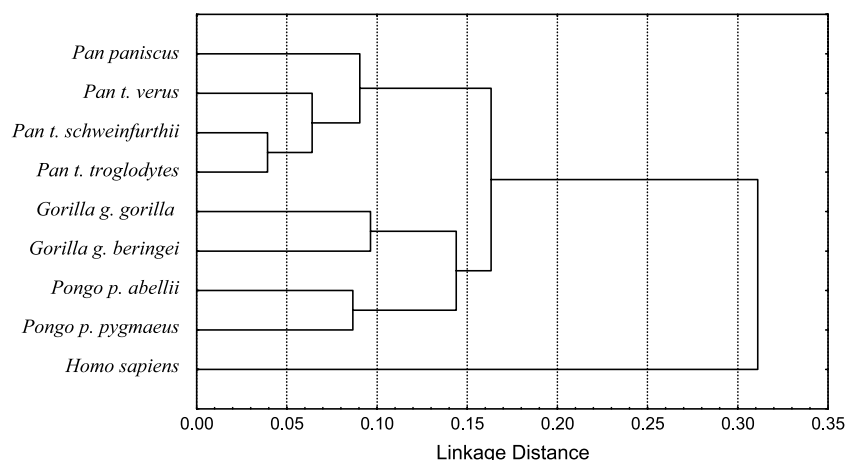

Fig. 4 Cluster analysis of all hominid subspecies using 48 principal components (explaining 99% of variance). UPGMA clustering, Euclidean distances.
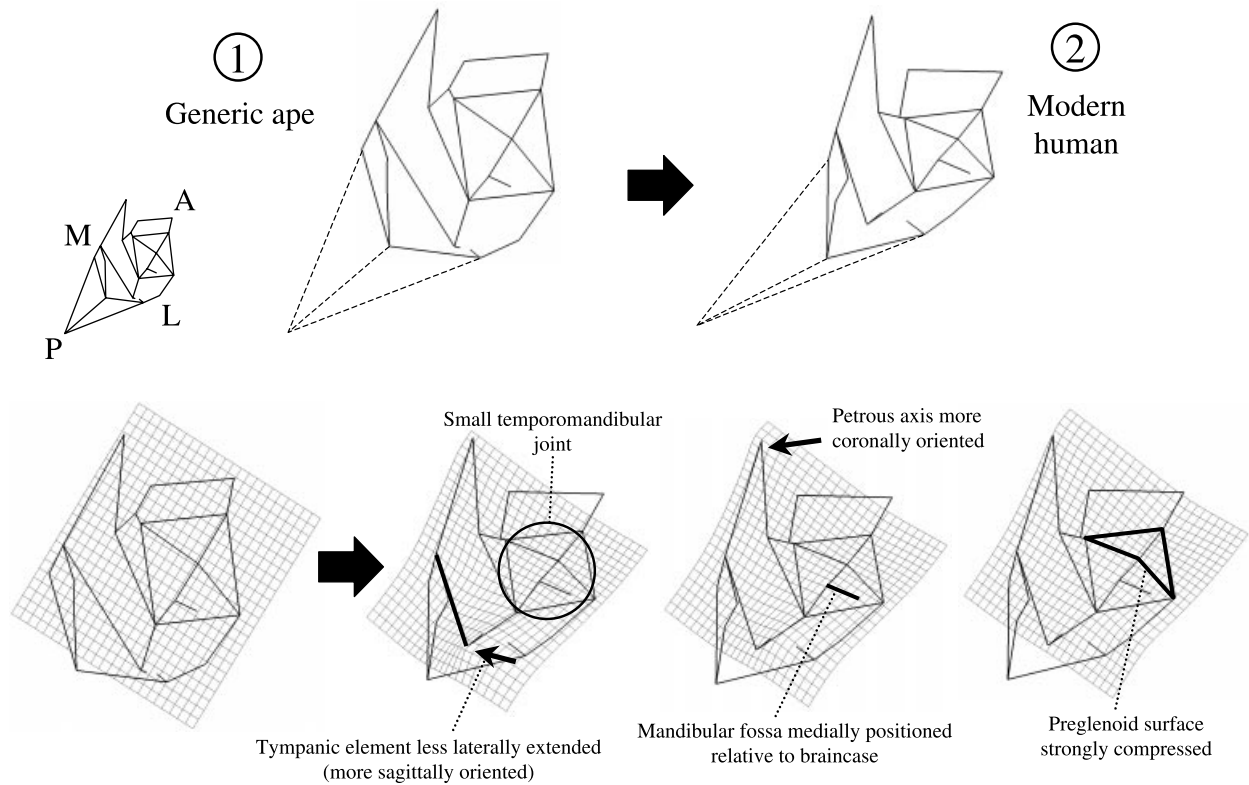
Fig. 5 Thin-plate spline transformation between apes and modern humans. Inferior view. Numbers correspond to those given in Fig. 3 and indicate the position of the reference and target shapes in the PCA. Dashed lines indicate the position of asterion, for display purposes. That landmark is not incorporated into the analysis. In this and all spline figures, different positions of the spline are shown, highlighting different aspects of the transformation. The labelled features are human traits.

inferior border (referred to by Weidenreich (1943) and most others as the petrous crest), and the vertical orientation of the tympanic element's anterior face. The human mastoid process is dramatically reconfigured relative to that of the great apes. Our analysis underscores the lateral placement of the human mastoid process (and corresponding reduction of its mediolateral width), as well as its pronounced inferior projection.

Principal component analysis of great ape species

Differences among great ape genera are clarified by excluding modern humans from the analysis. The first two PCs provide good discrimination among genera, and together explain 35.5% of the total variance (Fig. 7). Species within *Pan*, and subspecies within *Gorilla gorilla* and *Pongo pygmaeus*, are also distinguished to some extent by these components.

The third axis (6.5% of the variance) distinguishes between bonobos and chimpanzees, whereas subsequent axes reveal further differences between subspecies of

gorillas and orangutans. As with the analysis of the full hominid sample, there is no point at which eigenvalues clearly indicate that further axes are uninformative, although the first several axes, by definition, contain more information (Table 3).

In this analysis, all taxa are clearly distinct, but *Gorilla* and *Pongo* are slightly more similar to each other than either is to *Pan*. Chimpanzees are divergent in several ways, including the extensive preglenoid plane and the medially inflected mastoid process (see thin-plate spline comparisons below). As shown in Fig. 4, the differences between subspecies within *G. gorilla* or *Pongo pygmaeus* are similar in magnitude to those between the species *Pan troglodytes* and *P. paniscus*.

Thin plate spline comparison: *Pan* vs. other apes

In the PCA of apes only, differences among taxa are illustrated by a transformation along PC1, which depicts changes required to produce a chimpanzee-like form from one phenetically intermediate between
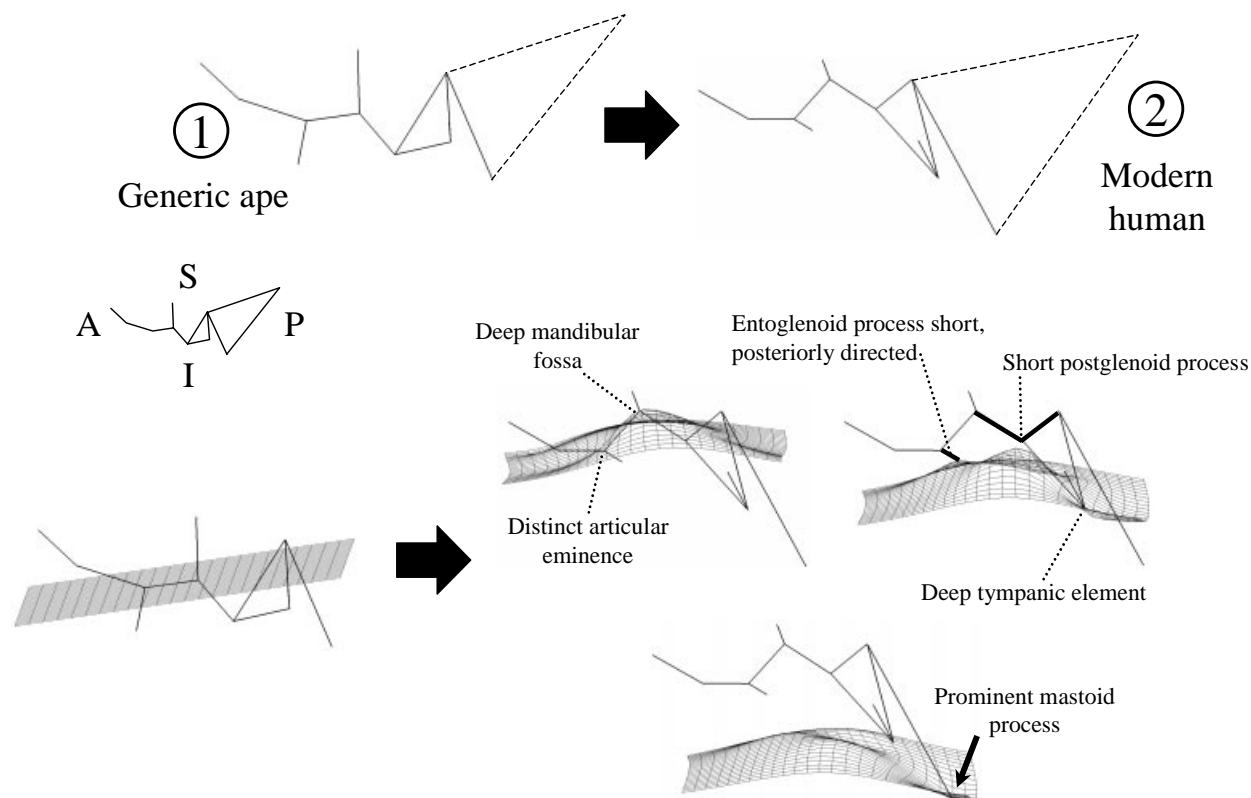
Fig. 6 Thin-plate spline transformation between apes and modern humans. Lateral view. Numbers correspond to those in Fig. 3 and indicate the position of the reference and target shapes in the principal component analysis. Dashed lines indicate the position of asterion, for display purposes. That landmark is not incorporated into the analysis. Some human characteristics are indicated.

gorillas and orangutans (Figs 8 and 9). These changes are more subtle than those required to produce human temporal bone morphology.

One characteristic of chimpanzees is that the tympanic element extends laterally to a lesser degree than in the other great apes. In this respect, *Pan* diverges slightly from the other great apes in the phenetic direction of *Homo*. Another similarity between *Pan* and *Homo* is the position of the mandibular fossa relative to the lateral wall of the braincase, indicated here by the wireframe extension segment from the mandibular fossa. Although this character has been hailed as a diagnostic feature of *Homo*, in comparison with great apes and *Australopithecus* (Hill et al. 1992), chimpanzees and humans share it. However, the medial placement of the mandibular fossa is due to different structural reasons in the two taxa. In humans, the braincase is expanded laterally, so that a greater portion of the mandibular fossa lies beneath it. In chimpanzees, the great thickness of the temporal squame causes the lateral wall of the braincase to be positioned far lateral to the sagittal plane of the

centre of the mandibular fossa (Sherwood et al. 2002). The 'medial placement of the mandibular fossa', phrased as such, is therefore probably not homologous in these taxa.

Unique chimpanzee characters strongly influence the transformations shown in Figs 8 and 9. These include an elongation of the anterior portion of the temporal bone and strong medial inflection of the mastoid process. The elongation of the anterior portion of the temporal bone results from an anterior extension of the temporomandibular joint capsule, which contrasts with the more restricted articular surface in gorillas and orangutans. The medial inflection of the mastoid process is related to minimal topographic relief of the process tip, so that its surface reaches nearly to the occipitomastoid suture in some individuals.

Figure 9 illustrates differences between chimpanzees and other apes in lateral view. In this view *Pan* has a shallower mandibular fossa, and a less inferiorly extensive postglenoid process, than either *Gorilla* or *Pongo*. The entoglenoid process is also weakly projecting, but

Table 4 Qualitative characters of the temporal bone (in alphabetical order) and their relationship to the multivariate analysis. The influence on principal components refers to the analysis of all hominoid taxa, and the signs are analogous to loading coefficients of eigenvectors. The morphocline of expression is derived from a consideration of all three principal components and summarizes the conditions for each taxon. This list of features is intended to facilitate comparison of this study to descriptive statements in the literature and is not exhaustive. All characters are expressions of shape, relative to the overall size of the temporal bone. Many of the characters are probably correlated

Character	Influence on principal components			Morphocline of expression		
	PC1	PC2	PC3	More		Less
Entoglenoid process (and foramen ovale) posteriorly positioned	N	N	+	*Pongo*		*Gorilla/Pan/Homo*
Entoglenoid process projection	+	−	−	*Gorilla*	*Pongo/Pan*	*Homo*
Entoglenoid process directed postero-inferiorly	−	N	N	*Homo*		*Gorilla/Pongo/Pan*
External acoustic porus relatively large	−	N	+	*Homo*	*Pongo/Pan*	*Gorilla*
Mandibular fossa depth (and prominence of articular eminence)	−	−	N	*Homo*	*Gorilla/Pongo*	*Pan*
Mandibular fossa medially positioned relative to lateral wall of braincase	−	+	N	*Homo/Pan*		*Gorilla/Pongo*
Mastoid process inferior projection	−	N	N	*Homo*		*Gorilla/Pongo/Pan*
Mastoid process medially inflected	+	+	N	*Pan*	*Gorilla/Pongo*	*Homo*
Mastoid process anterior projection	+	N	+	*Pongo*	*Gorilla/Pan*	*Homo*
Petrous axis more coronally orientated	−	N	N	*Homo*		*Gorilla/Pongo/Pan*
Postglenoid process size (inferior projection)	+	−	N	*Gorilla/Pongo*	*Pan*	*Homo*
Temporal bone mediolaterally narrow	−	N	N	*Homo*		*Gorilla/Pongo/Pan*
Temporal bone anteroposteriorly compressed	+	N	+	*Pongo*	*Gorilla/Pan*	*Homo*
Temporomandibular joint (TMJ) size (relative to temporal bone as a whole)	+	−	N	*Gorilla/Pongo*		*Homo/Pan*
TMJ shifted posterolaterally	N	N	+	*Pongo*		*Gorilla/Pan/Homo*
TMJ articular surface extends anteriorly (preglenoid plane)	+	+	N	*Pan*	*Gorilla/Pongo*	*Homo*
Tympanic wider anteroposteriorly in parasagittal plane of carotid canal	N	+	N	*Pan*		*Gorilla/Pongo/Homo*
Tympanic laterally projecting	+	N	−	*Gorilla*	*Pongo/Pan*	*Homo*
Tympanic depth (supero-inferior)	−	−	N	*Homo*	*Gorilla/Pongo*	*Pan*
Tympanic more sagittally orientated (axis from carotid canal to inferolateral point on tympanic)	−	N	+	*Homo*	*Pongo*	*Gorilla/Pan*
Tympanic and mastoid process more closely approximated	−	N	+	*Homo*	*Pongo*	*Gorilla/Pan*
Vertical thickness from mandibular fossa to supraglenoid surface	+	N	+	*Pongo*	*Gorilla/Pan*	*Homo*

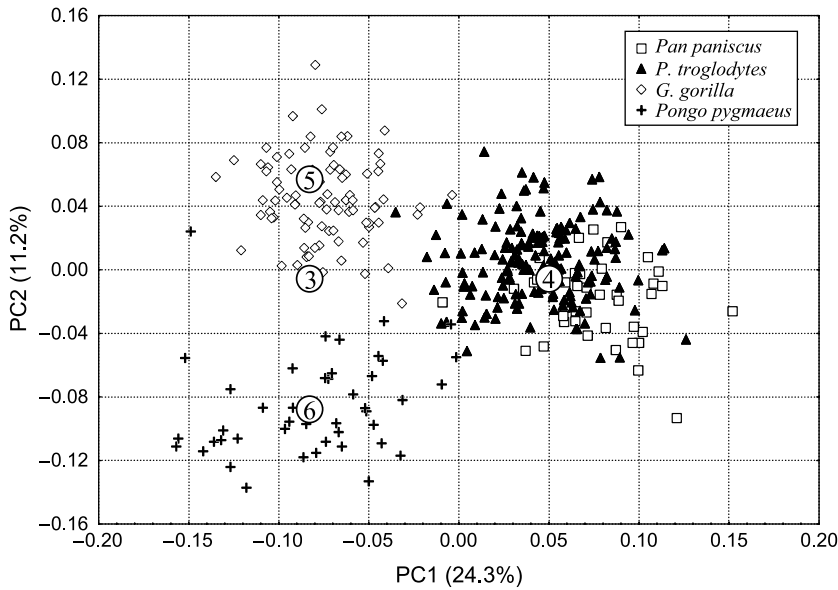Key: +, positively correlated with PC; −, negatively correlated with PC; N, no impact on PC.

Fig. 7 PCA of the great apes. The first two PCs summarize the differences among species. The numbered points are the reference and target shapes for the thin-plate spline transformations illustrated in Figs 9 and 10.
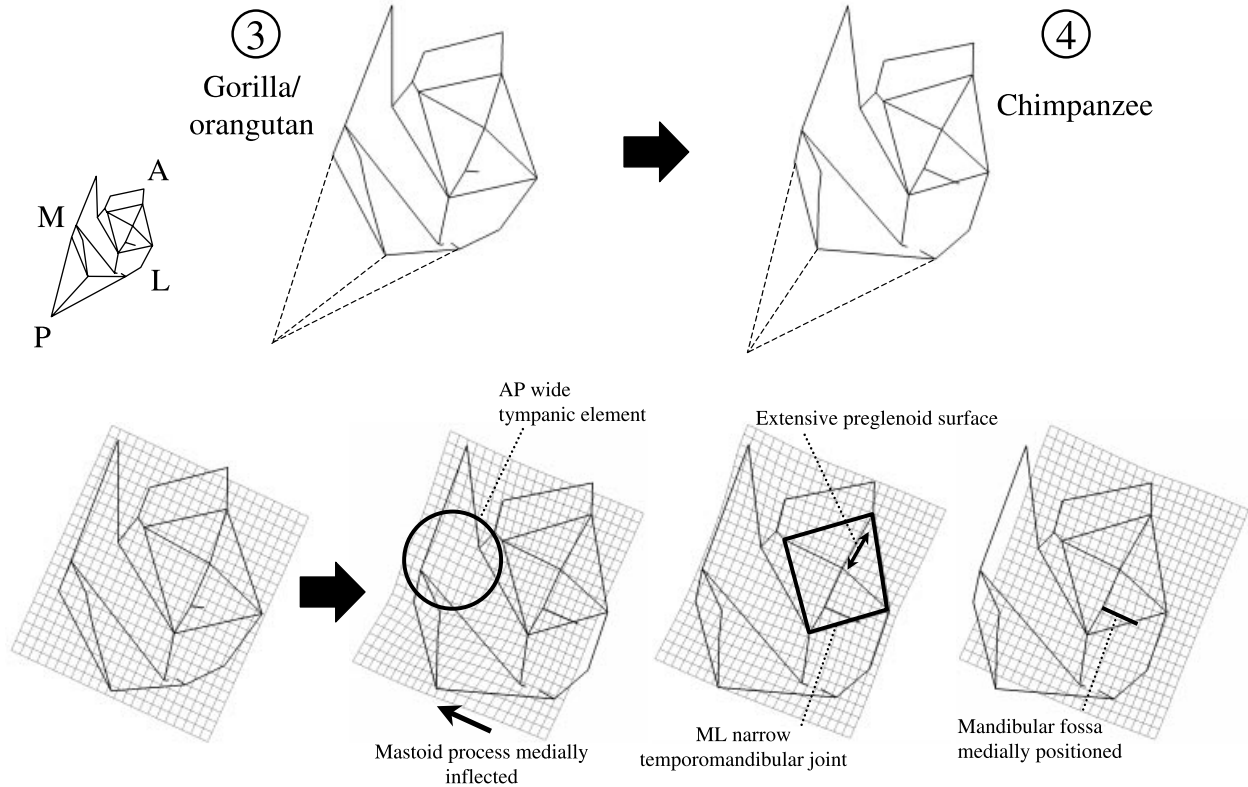

Fig. 8 Thin-plate spline transformation between a reference shape phenetically intermediate between *Gorilla* and *Pongo*, and a target shape at the *Pan troglodytes* centroid. Inferior view. Numbers correspond to those in Fig. 7 and indicate the position of the reference and target shapes in the PCA. Dashed lines indicate the position of asterion, for display purposes. That landmark is not incorporated into the analysis.

in this case *Pan* is similar to *Pongo*, and *Gorilla* is unique (see below). Finally, the mastoid process is relatively deeper (supero-inferiorly) in *Pan* than in other apes. While this may seem counter-intuitive, it is mainly due to the reduced topographic relief of other elements of the chimpanzee temporal bone. Thus, the mastoid is a relatively larger proportion of overall temporal bone size in *Pan*.
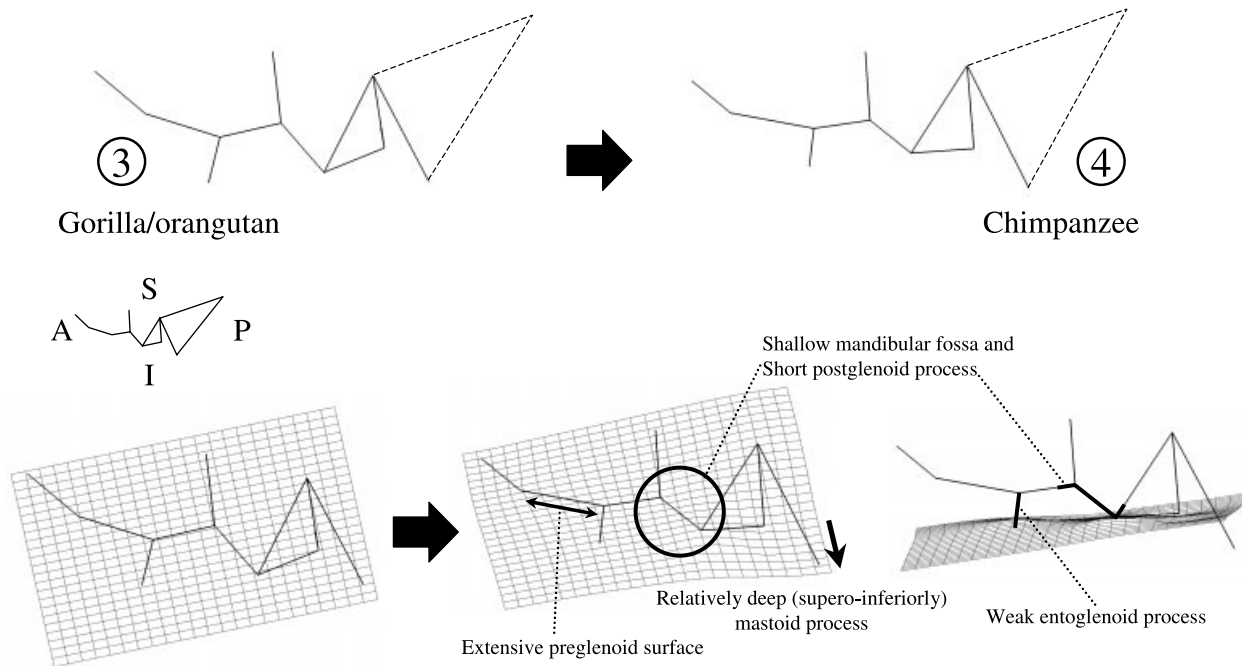
Fig. 9 Thin-plate spline transformation between a reference shape phenetically intermediate between *Gorilla* and *Pongo*, and a target shape at the *Pan* centroid. Lateral view. Numbers correspond to those in Fig. 7 and indicate the position of the reference and target shapes in the principal component analysis. Dashed lines indicate the position of asterion, for display purposes. That landmark is not incorporated into the analysis.

Thin plate spline comparison: *Gorilla* vs. *Pongo*

Differences between gorillas and orangutans are found primarily in the position of the temporomandibular joint and surrounding structures. At the same time, these taxa share several features related to the mastoid, petrous and tympanic elements of the temporal bone. These are summarized by comparisons with chimpanzees, presented above, and Tables 4 and 5.

In inferior view, orangutans are distinctive in the posterior position of the foramen ovale and the entoglenoid process, which are closer to the tympanic element, and a slightly more sagittal orientation of the tympanic axis (Fig. 10). The temporomandibular joint is shifted posterolaterally, and this has several effects on orangutan morphology. The overall distance from the articular eminence to the mastoid process is short, so that intervening structures are compressed. The mandibular fossa is an anteroposteriorly narrow groove, shown here by the close approximation of the centre of the mandibular fossa to the root of the postglenoid process. In many of these temporal bone characteristics, *Pongo* is unique among extant hominids (Table 4). *Gorilla* is unusual in the pronounced lateral extension of its tympanic element.

Table 5 Summary of qualitative character distributions among taxa

Number of characters unique to:	
Homo	17
Pongo	7
Pan	6
Gorilla	3
Number of characters shared by:	
Gorilla + *Pongo*	7
Gorilla + *Pan*	5
Gorilla + *Pongo* + *Pan*	4
Pongo + *Pan*	3
Homo + *Gorilla* + *Pan*	2
Homo + *Pan*	2
Homo + *Gorilla* + *Pongo*	1

This table summarizes the information available from the morphoclines listed in Table 4. Comparisons are entirely phenetic and underscore the patterns of similarity depicted by the phenogram in Fig. 4.

In lateral view (not illustrated), the orangutan stands out in the great thickness of the squamous temporal above the temporomandibular joint. In other words, the distance is greater from the mandibular fossa to the supraglenoid gutter. On the other hand, the gorilla entoglenoid process is more pronounced than in any other extant hominid taxon.
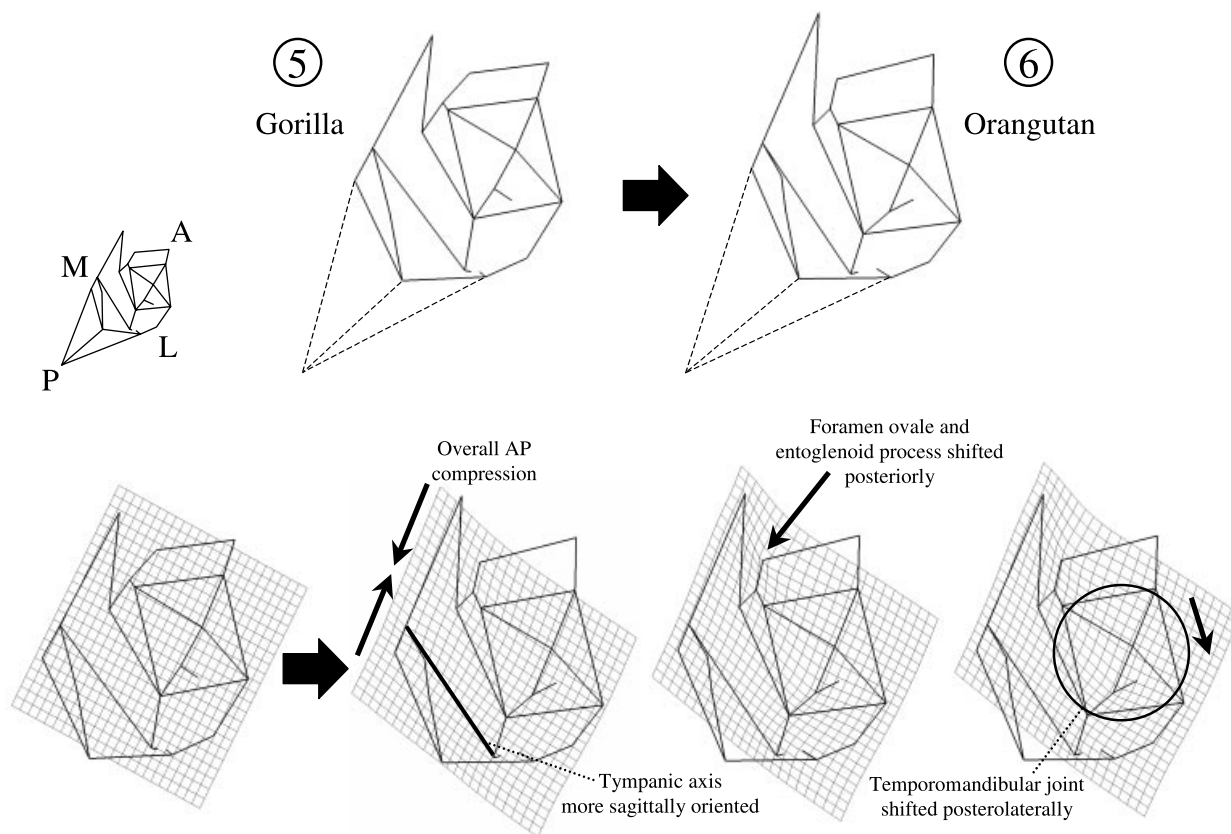
Fig. 10 Thin-plate spline transformation between *Gorilla* (reference shape) and *Pongo* (target shape). Inferior view. Numbers correspond to those in Fig. 7 and indicate the position of the reference and target shapes in the PCA. Dashed lines indicate the position of asterion, for display purposes. That landmark is not incorporated into the analysis.

Discussion

In this study, we have used geometric morphometrics to achieve two goals: quantification of morphological differences among hominid taxa and illustration of these differences using a method directly linked to the analysis of overall variation. Thin-plate spline and principal component analyses are clearly sensitive to aspects of hominid temporal bone form that have previously been described in qualitative or univariate terms, such as the size and shape of the temporomandibular joint.

The differences between humans and apes in temporal bone morphology highlight major trends in human evolution (Tables 4 and 5). For example, the mandibular fossa is deeper in humans, with a more pronounced articular eminence, and little if any anterior extension of the articular surface onto the preglenoid plane. These are traits commonly used in studies of hominin systematics (for an example of their use in a phylogenetic context, see Strait et al. 1997). Disagreements exist

as to how to quantify the size and shape of the glenoid articular surface (compare Ashton & Zuckerman, 1954; Picq, 1990; Wood, 1991; Tobias, 1991; Strait et al. 1997; and Martinez & Arsuaga, 1997). Our method, although integrative of numerous landmarks, probably corresponds most closely to that of Ashton & Zuckerman (1954). As they pointed out, the depth of the mandibular fossa depends on the gradient of the posterior slope of the articular eminence, not the height of the postglenoid process behind the fossa.

As the posterior slope of the articular eminence becomes steeper, and the eminence itself becomes more pronounced, it takes on a postero-inferior orientation, and in this way restricts anteroposterior movement of the mandibular condyle. This orientation is conveyed in our analysis by the orientation of the entoglenoid process, which is reoriented in the same manner as the articular eminence. In the great apes, however, the entoglenoid process is directed inferiorly, a marked difference from humans.

The anteroposterior compression of the human temporomandibular joint emphasized by Ashton & Zuckerman (1954) emerges in our study as well, and is especially evident in the relative size of the temporomandibular joint and associated structures. Wireframe diagrams and thin-plate spline transformations in Fig. 5 show that the joint surface is relatively small in humans. Correspondingly, the tympanic and mastoid elements of the temporal bone are relatively larger.

Dean & Wood (1981, 1982) describe the human cranial base as mediolaterally broad compared to great apes, noting that the distances between several bilateral landmarks (e.g. carotid canal) are greater in humans. The sole exception was the distance between the lateral edges of the tympanic elements. The mediolateral breadth of the human cranial base also relates to a more coronally orientated petrous element of the temporal bone. This feature is verified by our comparisons (Fig. 5).

However, our description of the human temporal bone as mediolaterally compressed would seem to contradict Dean & Wood's (1981) comparisons (see also Picq, 1990). This apparent contradiction has to do with the fact that their bilateral distances for the most part encompass space between the temporal bones. Thus, the spheno-occipital portion of the human cranial base is indeed relatively broad, as indicated by Dean & Wood's (1981) results. However, the temporal bone itself is mediolaterally narrow in many respects, including the temporomandibular joint, the tympanic element and the mastoid process. On the whole, this pattern can be summarized by describing the human temporal bones as narrow but laterally set on the cranial base. Only in the petrous axis itself can the human temporal bone be described as broad, for as this axis becomes more coronal, a greater portion of petrous length comes to lie in a mediolateral orientation. This is partly necessary to maintain articulation with the basioccipital, which is not especially wide in humans (Dean & Wood, 1981). Most other important differences between humans and great apes stem from the enhanced topographic relief of the temporal bone's basal aspect, which is manifest in the deep mandibular fossa, the vertically upright tympanic with distinct petrous crest, prominent vaginal and styloid processes and the mediolaterally narrow but inferiorly projecting mastoid process.

Unexpected aspects of our study include the findings on great ape variation conveyed by the principal component analyses. In most previous studies, chimpanzees and gorillas have been found to share quantitative aspects of cranial shape. On the basis of traditional cranial metrics, Shea (1983, 1985) concluded that many of the differences between gorillas and chimpanzees are the product of ontogenetic scaling. Using a combination of angles and linear dimensions, Dean & Wood (1981) noted the striking similarity in the arrangement of the chimpanzee and gorilla cranial bases. Aiello & Dean (1990, p. 68) stated that 'the morphology of the base of the great ape cranium varies surprisingly little between the gorilla, chimpanzee and orang-utan.' In a study of the temporomandibular joint, Picq (1990, e.g. pp. 131–132) contrasted 'grands singes' with 'homme moderne', de-emphasizing differences among great apes. These findings of similarity parallel studies that support a chimpanzee and gorilla clade (e.g. Andrews, 1992). Because genetic evidence generally favours a chimpanzee–human clade, cranial morphology has been interpreted by some as a poor source of phylogenetic evidence (Collard & Wood, 2000; but see Begun et al. 1997, for a contrary view).

A smaller number of researchers have focused on differences among great ape temporal bones (e.g. Ashton & Zuckerman, 1954). Our results underscore these differences. All genera are clearly distinct, with variation among genera occurring in the depth of the mandibular fossa, the form of the articular eminence, the configuration of tympanic and petrous elements, and the shape of the mastoid process. Some characters routinely treated as 'primitive' in studies of fossil hominins, such as a flat, anteriorly extensive glenoid articular surface, are actually found only in *Pan*.

On the whole, patterns of similarity in temporal bone shape support a phenetic grouping of gorillas and orangutans (Fig. 4, Tables 4 and 5). Expressed in another way, our findings on overall phenetic similarity contradict a gorilla–chimpanzee clade. While the phenetic tree presented in the analysis of all hominids is not rooted, it is clear that no rooting would rearrange the tree so that *Pan* and *Gorilla* are sister groups. It is noteworthy, on the other hand, that the phenetic tree is consistent with the phylogenetic tree that groups humans and chimpanzees in a clade based on the preponderance of genetic evidence. We do not wish to over-emphasize this consistency, however, because conclusions about the phylogenetic content of temporal bone morphometrics depend on the identification of primitive conditions for the great ape and human clade.

At this stage, we can hypothesize the primitive conditions for the hominine clade, i.e. the clade containing *Homo*, *Pan* and *Gorilla*. Because *Pongo* serves as an outgroup for the other three genera, the features shared by *Pongo* and *Gorilla* are probably primitive for hominines (Table 4). This, in turn, raises the likelihood that chimpanzees exhibit a significant number of autapomorphic temporal bone characters and a small number of synapomorphies shared with humans. In future work, these conclusions will be evaluated by studies of fossil hominids and the investigation of patterns of allometry in temporal bone shape.

Conclusions

This study confirms that geometric morphometrics effectively quantifies complex skeletal differences such as those found among hominid temporal bones. These methods also provide insight into the continuous variation that underlies many qualitative traits of the temporal bone.

The level of distinction between taxa in temporal bone morphology generally corresponds with expectations based on taxonomic rank and previous statements about group affinities based on cranial evidence. Thus the most pronounced differences are found between humans and all other taxa. Great ape subspecies are generally less distinct from each other than are species. However, the degree of difference among subspecies of *Gorilla gorilla* and *Pongo pygmaeus* approaches or exceeds that between *Pan troglodytes* and *P. paniscus*.

An unexpected result is the phenetic affinity of gorillas and orangutans, which, in contrast to chimpanzees, have deeper mandibular fossae, reduced anterior extension of the articular eminence, more projecting postglenoid processes, laterally positioned mastoid processes and relatively wider temporomandibular joints, among other characters. We hypothesize that these are primitive characteristics retained from the hominid common ancestor. This study emphasizes that African apes cannot be regarded as a monomorphic group in temporal bone morphology. Subsuming chimpanzees and gorillas into a single morphological group understates the diversity of extant hominid morphology.

Finally, if the characters shared by gorillas and orangutans are correctly interpreted as primitive, then the phenetic relationships presented here are consistent with a phylogenetic tree linking humans and chimpanzees as sister taxa. Some phylogenetic analyses

of morphology support this hypothesis, based on fossil evidence (e.g. Begun et al. 1997). Further evaluation of the phylogenetic implications of temporal bone anatomy requires inclusion of fossil taxa and is the subject of our ongoing study.

Acknowledgments

Endnotes

[1] As used here, Hominidae includes the genera *Homo*, *Pan, Gorilla* and *Pongo,* and all descendants of their common ancestor. Hominini includes modern humans and fossil taxa more closely related to them than to any other extant taxon.

[2] A bibliography of geometric morphometric techniques and case-studies within the natural sciences is available online at http://www.public.asu.edu/~jmlynch/ geomorph/.

[3] The dimensionality of registered coordinate space is $km - 7$, where k is the number of landmarks, and m is the number of dimensions (O'Higgins & Jones, 1998). Hence, PCA of registered coordinates will result in this number of principal components, given sufficient sample size.

References

Aiello LC, Dean MC (1990) *An Introduction to Human Evolutionary Anatomy*. London: Academic Press.

Andrews P (1992) Evolution and environment in the Hominoidea. *Nature* **360**, 641–646.

Ashton EH, Zuckerman S (1954) The anatomy of the articular fossa (fossa mandibularis) in man and apes. *Am. J. Phys. Anthropol.* **12**, 29–50.

Begun DR, Ward CV, Rose MD (1997) Events in hominoid evolution. In: *Function, Phylogeny, and Fossils* (eds Begun DR, Ward CV, Rose MD), pp. 389–415. New York: Plenum Press.

Bookstein FL (1989) Principal warps: thin-plate splines and the decomposition of deformations. *IEEE Transactions Pattern Anal. Machine Intelligence* **11**, 567–585.

Bookstein FL (1991) *Morphometric Tools for Landmark Data*. Cambridge: Cambridge University Press.

Braeuer G (1988) Osteometrie. In: *Anthropologie: Handbuch der Vergleichenden Biologie Des Menschen*. (eds Martin R, Knussmann R), pp. 160–232. Stuttgart: Gustav Fischer.

Clarke RJ (1977) *The Cranium of the Swartkrans Hominid, SK 847 and its Relevance to Human Origins*. PhD Thesis, Johannesburg: University of the Witwatersrand.

Collard M, Wood B (2000) How reliable are human phylogenetic hypotheses? *Proc. Natl. Acad. Sci. USA* **97**, 5003–5006.

Dean MC, Wood BA (1981) Metrical analysis of the basicranium of extant hominoids and *Australopithecus*. *Am. J. Phys. Anthropol.* **54**, 63–71.

Dean MC, Wood BA (1982) Basicranial anatomy of Plio-Pleistocene hominids from East and South Africa. *Am. J. Phys. Anthropol.* **59**, 157–174.

Dryden IL, Mardia KV (1993) Multivariate shape analysis. *Sankya* **55** (A), 460–480.

Dryden IL, Mardia KV (1998) *Statistical Shape Analysis*. London: John Wiley.

Goodall (1991) Procrustes methods in the statistical analysis of shape. *J. Royal Statist. Soc.* **53**, 285–339.

Hennessy RJ, Stringer CB (2002) Geometric morphometric study of the regional variation of modern human craniofacial form. *Am. J. Phys. Anthropol.* **117**, 37–48.

Hill A, Ward S, Deino A, Curtis G, Drake R (1992) Earliest *Homo*. *Nature* **355**, 719–722.

Immersion Corporation (1998) *Microscribe 3D User's Guide*. San Jose, CA: Immersion Corporation.

Kendall DG (1984) Shape manifolds, Procrustean metrics and complex projective spaces. *Bull. London Mathemat. Soc.* **16**, 81–121.

Kimbel WH, Rak Y (1993) The importance of species taxa in paleoanthropology and an argument for the phylogenetic concept of the species category. In: *Species, Species Concepts, and Primate Evolution* (eds Kimbel WH, Martin LB), pp. 461–484. New York: Plenum Press.

Kimbel WH, White TD (1988) Variation, sexual dimorphism and the taxonomy of *Australopithecus*. In: *Evolutionary History of the 'Robust' Australopithecines* (ed. Grine FE), pp. 175–192. New York: Aldine de Gruyter.

Kimbel WH, White TD, Johanson DC (1984) Cranial morphology of *Australopithecus afarensis*: a comparative study based on a composite reconstruction of the adult skull. *Am. J. Phys. Anthropol.* **65**, 337–388.

Le Gros Clark WE (1947) Observations on the anatomy of the fossil Australopithecinae. *J. Anat.* **81**, 300–333.

de Leon MSP, Zollikofer CPE (2001) Neanderthal cranial ontogeny and its implications for late hominid diversity. *Nature* **412**, 534–538.

Lockwood CA, Lynch JM, Kimbel WH (2000) Establishing the polarity of temporal bone morphology in African hominoids using geometric morphometrics. *Am. J. Phys. Anthropol. Suppl.* **30**, 212.

Lockwood CA, Tobias PV (1999) A large male hominin cranium from Sterkfontein, South Africa, and the status of *Australopithecus africanus*. *J. Hum. Evol.* **36**, 637–685.

Lynch JM, Wood CG, Luboga SA (1996) Geometric morphometrics in primatology: craniofacial variation in *Homo sapiens* and *Pan troglodytes*. *Folia Primatol.* **67**, 15–39.

Marcus LF, Corti M, Loy A, Naylor G, Slice DE, eds. (1996) Advances in Morphometrics. NATO ASI Series A, Vol. 284. New York: Plenum Press.

Martinez I, Arsuaga JL (1997) The temporal bones from Sima de los Huesos Middle Pleistocene site (Sierra de Ata puerca, Spain): a phylogenetic approach. *J. Hum. Evol.* **33**, 283–318.

O'Higgins P, Jones N (1998) Facial growth in *Cercocebus torquatus*: an application of three dimensional geometric morphometric techniques to the study of morphological variation. *J. Anat.* **193**, 251–272.

O'Higgins P (2000) The study of morphological variation in the hominid fossil record: biology, landmarks and geometry. *J. Anat.* **197**, 103–120.

O'Higgins P, Chadfield P, Jones N (2001) Facial growth and the ontogeny of morphological variation within and between the primates *Cebus apella* and *Cercocebus torquatus*. *J. Zool.* **254**, 337–357.

Olson TR (1981) Basicranial morphology of the extant hominids and Pliocene hominids: the new material from the Hadar Formation, Ethiopia, and its significance in early human evolution and taxonomy. In: *Aspects of Human Evolution* (ed. Stringer CB), pp. 99–128. London: Taylor & Francis.

Olson TR (1985) Cranial morphology and systematics of the Hadar formation hominids and 'Australopithecus' africanus. In: *Ancestors: the Hard Evidence* (ed. Delson E), pp. 102–119. New York: Alan R. Liss.

Penin X, Berge C (2001) Heterochronies and procrustes superimposition: application to the skulls of primates Hominoidea. *C. R. Acad. Sci. Series* **III** (324), 87–93.

Picq P (1984) L'articulation temporo-mandibulaire des fossiles du genre *Homo* du Plio-Pleistocene de l'Afrique de l'Est. *C. R. Acad. Sci. Series* **II** (298), 501–506.

Picq P (1985) L'articulation temporo-mandibulaire d'*Australopithecus afarensis*. *C. R. Acad. Sci. Series* **II** (300), 469–474.

Picq P (1990) *L'Articulation Temporo-mandibular des Hominides. Biomecanique, Allometrie, Anatomie Comparee et Evolution*. Cahiers de Paleontologie (Paleoanthropologie). Paris: Editions du CNRS.

Rohlf FJ, Slice DE (1990) Extensions on the Procrustes method for the optimal superimposition of landmarks. *Syst. Zool.* **39**, 40–59.

Rohlf FJ (1999) Shape statistics: Procrustes superimpositions and tangent spaces. *J. Classification* **16**, 197–223.

Rohlf FJ (2000a) On the use of shape spaces to compare morphometric methods. *Hystrix It. J. Mamm. (N.S.)* **11**, 8–24.

Rohlf FJ (2000b) Statistical power comparisons among alternative morphometric methods. *Am. J. Phys. Anthropol.* **111**, 463–478.

Rosas A, Bastir M (2002) Thin-plate spline analysis of allometry and sexual dimorphism in the human craniofacial complex. *Am. J. Phys. Anthropol.* **117**, 236–245.

Shea BT (1983) Paedomorphosis and neoteny in the pygmy chimpanzee. *Science* **222**, 521–522.

Shea BT (1985) Ontogenetic allometry and scaling: a discussion based on the growth and form of the skull of African apes. In: *Size and Scaling in Primate Biology* (ed. Jungers WL), pp. 175–205. New York: Plenum Press.

Sherwood RJ, Ward SC, Hill A (2002) The taxonomic status of the Chemeron temporal (KNM-BC 1). *J. Hum. Evol.* **42**, 153–184.

Strait DS, Grine FE, MoniZ MA (1997) A reappraisal of early hominid phylogeny. *J. Hum. Evol.* **32**, 17–82.

Tobias PV (1967) *Olduvai Gorge*, *Vol. II. The Cranium and Maxillary Dentition of* Australopithecus (Zinjanthropus) boisei. London: Cambridge University Press.

Tobias PV (1991) *Olduvai Gorge, Vol. IV. The Skulls, Endocasts and Teeth of* Homo habilis. London: Cambridge University Press.

Weidenreich F (1943) The skull of *Sinanthropus pekinensis*: a comparative odontography of the hominids. *Palaeontol. Sin., New Series D* **10**, 1–484.

Weidenreich F (1948) *About the Morphological Character of the Australopithecine Skull*, pp. 153–158. Cape Town: Royal Society of South Africa.

White TD, Johanson DC, Kimbel WH (1981) *Australopithecus africanus*: its phylogenetic position reconsidered. *S. Afr. J. Sci.* **77**, 445–470.

Wood BA (1991) *Koobi Fora Research Project IV: Hominid Cranial Remains from Koobi Fora*. Oxford: Clarendon Press.

Wood CG, Lynch JM (1996) Sexual dimorphism in the craniofacial skeleton of modern humans. In: *Advances in Morphometrics* (eds Marcus LF, Corti M, Loy A, Naylor G, Slice DE), pp. 407–414. New York: Plenum Press.

Yarroch LA (1996) Shape analysis using the thin-plate spline: Neanderthal cranial shape as an example. *Yrbk. Phys. Anthropol.* **39**, 43–89.